Discrete diffraction and spatial gap solitons in photovoltaic $LiNbO_3$ waveguide arrays

Feng Chen, Milutin Stepić, Christian E. Rüter, Daniel Runde, Detlef Kip

Institute of Physics and Physical Technologies, Clausthal University of Technology, 38678 Clausthal-Zellerfeld, Germany
detlef.kip@tu-clausthal.de

Vladimir Shandarov

State University of Control Systems and Radioelectronics, 40 Lenin Ave., 634050 Tomsk, Russia

Ofer Manela, Mordechai Segev

Department of Physics, Solid State Institute, Technion, 32000 Haifa, Israel

Abstract: We investigate, experimentally and theoretically, light propagation in one-dimensional waveguide arrays exhibiting a saturable self-defocusing nonlinearity. We demonstrate low-intensity "discrete diffraction", and the high-intensity formation of spatial gap solitons arising from the first band of the transmission spectrum. The waveguide arrays are fabricated by titanium in-diffusion in a photorefractive copper-doped lithium niobate crystal, and the optical nonlinearity arises from the bulk photovoltaic effect.

© 2005 Optical Society of America

OCIS codes: (230.7330) Waveguides; (190.4420) Nonlinear optics, transverse effect in; (190.5530) Pulse propagation and solitons; (999.9999) Photonic lattices

References and links

1. D. N. Christodoulides, F. Lederer, and Y. Silberberg, "Discretizing light behavior in linear and nonlinear waveguide lattices," Nature **424**, 817–823 (2003).
2. D. N. Christodoulides and R. I. Joseph, "Discrete self-focusing in nonlinear arrays of coupled waveguides," Opt. Lett. **19**, 794–796 (1988).
3. H. S. Eisenberg, Y. Silberberg, Y. Morandotti, R. Boyd, and J. S. Aitchison, "Discrete spatial optical solitons in waveguide arrays," Phys. Rev. Lett. **81**, 3383–3386 (1998).
4. Y. S. Kivshar, "Self-localization in arrays of defocusing waveguides," Opt. Lett. **20**, 1147–1149 (1993).
5. J. Feng, "Alternative scheme for studying gap solitons in infinite periodic Kerr media," Opt. Lett. **20**, 1302–1304 (1993).
6. J. W. Fleischer, T. Carmon, M. Segev, N. K. Efremidis, and D. N. Christodoulides, "Observation of discrete solitons in optically induced real time waveguide arrays," Phys. Rev. Lett. **90**, 023902 (2003).
7. J. W. Fleischer, M. Segev, N. K. Efremidis, and D. N. Christodoulides, "Observation of two-dimensional discrete solitons in optically induced nonlinear photonic lattices," Nature **422**, 147–150 (2003).
8. S. Darmanyan, A. Kobyakov, and F. Lederer, "Stability of strongly localized excitations in discrete media with cubic nonlinearity," JETP **86**, 682–686 (1998).
9. D. Neshev, E. Ostrovskaya, Y. Kivshar, and W. Krolikowski, "Spatial solitons in optically induced gratings," Opt. Lett. **28**, 710–712 (2003).
10. O. Manela, O. Cohen, G. Bartal, J. W. Fleischer, and M. Segev, "Two-dimensional higher-band vortex lattice solitons," Opt. Lett. **29**, 2049–2051 (2004).
11. G. Bartal, O. Manela, O. Cohen, J. W. Fleischer, and M. Segev, "Observation of 2nd-band vortex solitons in 2D photonic lattices," submitted to Phys. Rev. Lett.
12. D. Mandelik, H. S. Eisenberg, Y. Silberberg, R. Morandotti, and J. S. Aitchison, „Band-gap structure of waveguide arrays and excitation of Floquet-Bloch solitons," Phys. Rev. Lett. **90**, 053902 (2003).
13. O. Cohen, T. Schwartz, J. W. Fleischer, M. Segev, and D. N. Christodoulides, "Multiband vector lattice solitons," Phys. Rev. Lett. **91**, 113901 (2003).

#6929 - $15.00 US Received 22 March 2005; revised 18 May 2005; accepted 24 May 2005
(C) 2005 OSA

14. A. A. Sukhorukov and Y.S. Kivshar, "Multigap discrete vector solitons," Phys. Rev. Lett. **91**, 113902 (2003).
15. Y. V. Kartashov, V. A. Vysloukh, L. Torner, "Soliton trains in photonic lattices," Opt. Express **12**, 2831–2837 (2004).
16. A. S. Davydov, *Solitons in Molecular Systems* (Kluwer Academic, Dordrecht, 1991).
17. A. H. Xie, L. van der Meer, V. Hoff, and R. H. Austin, "Long-lived amide I vibrational modes in myoglobin," Phys. Rev. Lett. **84,** 5435–5438 (2000).
18. B. I. Swanson J. A. Brozik, S. P. Love, G. F. Strouse, A. P. Shreve, A. R. Bishop W.-Z. Wang, and M. I. Salkola, "Observation of intrinsically localized modes in a discrete low-dimensional material," Phys. Rev. Lett. **82**, 3288–3291 (1999).
19. U. T. Schwartz, L. Q. English, and A. J. Sievers, "Experimental generation and observation of intrinsic localized spin wave modes in an antiferromagnets," Phys. Rev. Lett. **83**, 223–226 (1999).
20. E. Trias, J. J. Mazo, and T. P. Orlando, "Discrete breathers in nonlinear lattices: experimental detection in Josephson junctions," Phys. Rev. Lett. **84**, 741–744 (2000).
21. P. Binder, D. Abraimov, A. V. Ustinov, S. Flach, and Y. Zolotaryuk, "Observation of breathers in Josephson ladders," Phys. Rev. Lett. **84**, 745–748 (2000).
22. A. Trombettoni and A. Smerzi, "Discrete solitons and breathers with dilute Bose-Einstein condensates," Phys. Rev. Lett. **86**, 2353–2356 (2001).
23. B. Eiermann, Th. Anker, M. Albiez, M. Taglieber, P. Treutlein, K.-P. Marzlin, and M. K. Oberthaler, "Bright Bose-Einstein gap solitons of atoms with repulsive interaction," Phys. Rev. Lett. **92**, 230401 (2004).
24. D. Mandelik, R. Morandotti, J. S. Aitchison, and Y. Silberberg, "Gap solitons in waveguide arrays," Phys. Rev. Lett. **92,** 093904 (2004).
25. D. N. Neshev, A. A. Sukhorukov, B. Hanna, W. Krolikowski, and Y. S. Kivshar, "Controlled generation and steering of spatial gap solitons," Phys. Rev. Lett. **93**, 083905 (2004).
26. M. Segev, G. C. Valley, B. Crosignani, P. D. Porto, and A. Yariv, "Steady-state spatial screening solitons in photorefractive materials with external applied field," Phys. Rev. Lett. **73**, 3211–3214 (1994).
27. N. K. Efremidis S. Sears, D. N. Christodoulides, J. W. Fleischer, and M. Segev, "Discrete solitons in photorefractive optically induced photonic lattices," Phys. Rev. E **66**, 046602 (2002).
28. J. Meier, J. Hudock, D. N. Christodoulides, G. Stegeman, Y. Silberberg, R. Morandotti, and J. S. Aitchison, "Discrete vector solitons in Kerr nonlinear waveguide arrays," Phys. Rev. Lett. **91**, 143907 (2003).
29. S. Orlov, A. Yariv, and M. Segev, "Nonlinear self-phase matching of optical second harmonic generation in lithium niobate," Appl. Phys. Lett. **68**, 1610–1612 (1996).
30. M. Segev, B. Crosignani, A. Yariv, and B. Fischer, "Spatial solitons in photorefractive media," Phys. Rev. Lett. **68**, 923–926 (1992).
31. M. Segev, B. Crosignani, P. DiPorto, G. C. Valley, and A. Yariv, "Steady state spatial screening-solitons in photorefractive media with external applied field," Phys. Rev. Lett. **73**, 3211–3214 (1994).
32. G. C. Valley, M. Segev, B. Crosignani, A. Yariv, M. Fejer, and M. Bashaw, "Bright and dark photovoltaic spatial solitons," Phys. Rev. A **50**, R4457–R4460 (1994).
33. G. Duree, J. Shultz, G. Salamo, M. Segev, A. Yariv, B. Crosignani, P. DiPorto, E. Sharp, and R. R. Neurgaonkar, "Observation of self-trapping of an optical beam due to the photorefractive effect," Phys. Rev. Lett. **71**, 533–536 (1993).
34. M. Taya, M. Bashaw, M. Fejer, M. Segev, and G. C. Valley, "Observation of dark photovoltaic spatial solitons," Phys. Rev. A **52**, 3095–3100 (1995).
35. Z. Chen, M. Segev, D. W. Wilson, R. E. Muller, and P. D. Maker, „Self-trapping of an optical vortex by use of the bulk photovoltaic effect," Phys. Rev. Lett. **78**, 2948–2951 (1997).
36. J. W. Fleischer, G. Bartal, O. Cohen, O. Manela, M. Segev, J. Hudock, and D. N. Christodoulides, "Observation of vortex-ring 'discrete' solitons in 2D photonic lattices," Phys. Rev. Lett. **92**, 123904 (2004).
37. D. N. Neshev, T. J. Alexander, E. A. Ostrovskaya, Y. S. Kivshar, H. Martin, I. Makasyuk, and Z. Chen, "Observation of discrete vortex solitons in optically induced photonic lattices," Phys. Rev. Lett. **92**, 123903 (2004).
38. O. Cohen, G. Bartal, H. Buljan, T. Carmon, J. W. Fleischer, M. Segev, and D. N. Christodoulides, "Observation of random-phase lattice solitons," Nature **433**, 500–503 (2005).
39. H. Martin, E. D. Eugenieva, Z. Chen, and D. N. Christodoulides, "Discrete solitons and soliton-induced dislocations in partially coherent photonic lattices," Phys. Rev. Lett. **92**, 123902 (2004).
40. Z. Chen, H. Martin, E. D. Eugenieva, J. Xu, and A. Bezryadina, "Anisotropic enhancement of discrete diffraction and formation of two-dimensional discrete-soliton trains," Phys. Rev. Lett. **92**, 143902 (2004).
41. J. Yang, I. Makasynk, A. Bezryadina, and Z. Chen, "Dipole solitons in optically-induced two-dimensional photonic lattices," Opt. Lett. **29**, 1662–1664 (2004).
42. Z. Chen, A. Bezryadina, I. Makasynk, and J. Yang, "Observation of two-dimensional vector lattice solitons," Opt. Lett. **29**, 1656–1658 (2004).
43. M. Stepic, D. Kip, Lj. Hadzievski, and A. Maluckov, "One-dimensional bright discrete solitons in media with saturable nonlinearity," Phys. Rev. E **69**, 066618 (2004).
44. K. Peithmann, J. Hukriede, K. Buse, and E. Krätzig: "Photorefractive properties of lithium niobate volume crystals doped by copper diffusion," Phys. Rev. B **61**, 4615–4620 (2000).
45. H. Yoshida, "Construction of higher order sympletic integrators," Phys. Lett. A **150**, 262–269 (1990).

#6929 - $15.00 US Received 22 March 2005; revised 18 May 2005; accepted 24 May 2005
(C) 2005 OSA

46. H. S. Eisenberg, Y. Silberberg, R. Morandotti, and J. S. Aitchison: "Diffraction management," Phys. Rev. Lett. **85**, 1863–1866 (2000).
47. T. Pertsch, U. Peschel, F. Lederer, J. Burghoff, M. Will, S. Nolte, and A. Tünnermann, "Discrete diffraction in two-dimensional arrays of coupled waveguides in silica," Opt. Lett. **29**, 468–470 (2004).
48. The long response time is a result of the Cu doping and the low photoconductivity of our sample. Very recently we have fabricated samples with Fe doping where the response time can be shortened to about 100 s.
49. M. Segev, G. C. Valley, M. C. Bashaw, M. Taya, and M. M. Fejer, "Photovoltaic spatial solitons," J. Opt. Soc. Am. B **14**, 1772–1781 (1997).

1. Introduction

The past few years have witnessed a strong interest in periodic optical systems, such as waveguide arrays, photonic lattices, and photonic crystals. Such systems exhibit many attractive features for which no counterpart exists in homogeneous media, including forbidden gaps in their transmission spectra, Bragg diffraction, and the exciting possibility of controlling diffraction (for an updated review see Ref. [1]). Of particular interest are the nonlinear periodic systems, which support self-localized structures called lattice solitons, also known as "discrete solitons" [2,3]. As expected from such periodic systems, many of the soliton phenomena found in them cannot exist in homogeneous nonlinear media. That includes, for example, spatial gap solitons [4-7], dipole-like ("twisted") solitons [8,9], higher-band solitons [10,11] and breathers [12], multi-band solitons [13,14], soliton trains [15], to name a few. The phenomena of lattice solitons (solitons in periodic structures) is in fact universal, manifesting itself in a variety of systems in nature, from biological molecules [16,17], to charge density waves [18], spin waves [19], arrays of Josephson junctions [20,21], and very recently in Bose-Einstein condensates [22,23].

A characteristic benchmark experiment in such nonlinear periodic systems involves exciting a single channel by a narrow wavepacket (beam of light), watch the wavepacket broaden at low power, as it experiences linear lattice diffraction, and then observing it narrow down and self-trap at sufficiently high power that activates the proper nonlinearity supporting lattice solitons [3]. Such experiments have been carried out with wavepackets launched at the base of the 1st Brilluoin zone [3], where normal diffraction is balanced by self-focusing, and later on at the edge of the 1st Brilluoin zone where anomalous diffraction is counteracted by self-defocusing, giving rise to spatial gap solitons [6,7]. Subsequent experiments have demonstrated gap solitons arising from the second band [23,24]. Thus far, however, spatial optical gap solitons have been demonstrated in only two physical systems: photorefractives [6,7,25] displaying the screening nonlinearity [26] in which waveguides are optically induced [27], and fabricated GaAs waveguides possessing the optical Kerr nonlinearity [24,28].

Here, we demonstrate, experimentally and theoretically, spatial gap solitons in one-dimensional (1D) waveguide arrays exhibiting a saturable self-defocusing nonlinearity. The waveguide arrays are fabricated by titanium in-diffusion in a copper-doped lithium niobate ($LiNbO_3$) crystal, and the optical nonlinearity arises from the bulk photovoltaic effect. The maximum nonlinear index change induced by the photovoltaic nonlinearity is typically very high (~0.003 [29]), and the index contrast of the fabricated waveguide array can be adjusted over a wide range. Our experiments, therefore, offer a new physical system supporting lattice (gap) solitons, offering a strong saturable nonlinearity along with the robustness of the fabricated structures.

The physical nonlinearity that may cause soliton formation in inorganic photorefractive media includes two different charge transport mechanisms: the drift mechanism in an externally applied electric field [30,31], and the bulk photovoltaic (photogalvanic) effect that leads to an internal electric field [32]. In bulk photorefractives, solitons supported by either one of these mechanisms have been observed since 1993 [33] and 1995 [34,35], respectively. Since then, such screening solitons and photovoltaic solitons have been demonstrated in many photorefractive materials. More recently, following the suggestion of the optical induction

#6929 - $15.00 US Received 22 March 2005; revised 18 May 2005; accepted 24 May 2005
(C) 2005 OSA

technique [27], the photorefractive screening nonlinearity has become a major player in lattice soliton experiments [6,7,9,11,25,36-42]. However, thus far the ability to employ the photovoltaic nonlinearity for lattice soliton experiments was left behind, even though $LiNbO_3$ crystals exhibiting such nonlinearity are a fairly mature technology. Namely, $LiNbO_3$ crystals doped with certain metal ions (e.g., copper or iron) exhibit strong photovoltaic effects, which lead to a nonlinear index change of a saturable self-defocusing nature. At the same time, single mode waveguide arrays in $LiNbO_3$ can be fabricated through the extensively used titanium in-diffusion method. Nonetheless, soliton lattice experiments in photovoltaic waveguide arrays have thus far not been reported. With this idea in mind, a recent theoretical paper [43] has shown that discrete solitons can exist in such waveguide arrays with a saturable self-defocusing nonlinearity. Here we present the experimental observation of spatial gap solitons in photovoltaic 1D waveguide arrays in $LiNbO_3$, possessing optical power as low as several microwatts.

2. Experimental methods

The waveguide arrays are prepared in two steps, using *x*-cut $LiNbO_3$ wafers of congruently melting composition supplied by Crystal Technology Inc. In the first step, the substrates with dimensions of $1 \times (10–25) \times 7.8$ mm^3 along the crystallographic *x*, *y*, *z* axes are doped with copper ions to increase the photorefractive effect. The ferroelectric *c*-axis points along the *z*-direction. A thin copper layer of 20 nm thickness is vacuum-deposited on top of the substrate and in-diffused for 2 hours at 1000 °C in a wet argon atmosphere. For a total diffusion time of 4 hours (this time includes the additional titanium in-diffusion of another 2 hours, see description below), a nearly constant copper concentration of 5×10^{24} m^{-3} is obtained at the surface region. Alternatively, to avoid the increase in surface roughness caused by copper in-diffusion, copper may be also in-diffused from the back side of the crystal. For that, a 70 nm-thick layer of copper is in-diffused for 24 hours. In this case the concentration beneath the surface is again 5×10^{24} m^{-3}.

In the second step, a 10 nm-thin titanium layer is deposited on the top-side by sputtering, and is structured using standard lithographic techniques. In this way, we fabricate a grating of period $\Lambda = 8.4$ μm, consisting of 4 μm-wide titanium stripes orientated parallel to the *y*-axis of the substrate and separated by 4.4 μm. Subsequently the stripes are in-diffused for 2 hours at 1000 °C in air. The titanium increases the refractive index of the $LiNbO_3$ substrate and gives rise to waveguiding in its vicinity. Each separate channel forms a single-mode waveguide for TE polarized light of wavelength 514.5 nm. Each such channel is evanescently coupled to its nearest neighbours. The corresponding coupling constant is given by the overlap integral of the modes with the index profile and has been calculated to be ≈1 mm^{-1}.

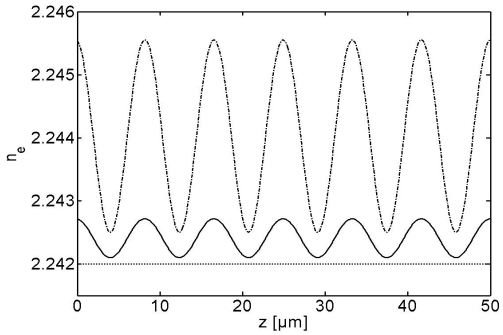

Fig. 1. Refractive index profiles $n(z)$ of a $LiNbO_3$ waveguide array at two different depths of the in-diffused structures: at the depth of maximum field amplitude of the modes (dash-dotted line) and at a depth where the amplitude has dropped by a factor 1/*e* (solid line). The substrate refractive index is 2.242 (dotted line at the bottom).

#6929 - $15.00 US Received 22 March 2005; revised 18 May 2005; accepted 24 May 2005
(C) 2005 OSA

We calculate the diffusion profile by solving Fick's law for a finite source in two dimensions. As a result of the in-diffusion from the substrate surface, the corresponding periodic refractive index profile is a function of depth with the strongest modulation at the surface for $x = 0$. Figure 1 shows the calculated periodic index potential $n(z) = n(z + \Lambda)$ at the depth below the surface where the maximum amplitude of the modes occurs and at the depth where the modal amplitude has dropped by a factor 1/*e*. For the theoretical modelling in the next section, the index profiles are fairly well approximated by a $\cos^2$ function, which yields the profile $n(z) = 2.242 + 0.00052\cos^2(\pi z/\Lambda)$ for a depth close to the one where the intensity of the waveguide mode has its "center of gravity".

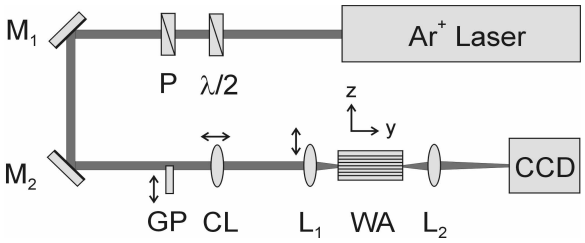

Fig. 2. Experimental set-up: *P*, polarizer; $\lambda/2$, half-wave plate; $M_{1,2}$, mirrors; *GP*, thin glass plate; *CL*, cylindrical lens; $L_{1,2}$, microscope lenses; *WA*, waveguide array; *CCD*, CCD camera. The light source is a 514.5 nm wavelength argon ion laser.

Figure 2 shows the experimental set-up. We use the green line (wavelength $\lambda = 514.5$ nm) of an argon ion laser as our light source. A combination of half-wave plate $\lambda/2$ and polarizer *P* allows for precise adjustment of power and polarization of the light. We first install a thin tilted glass plate (denoted as *GP*) into half of the optical beam, so as to retard the phase of one half of the beam by π with respect to the other half, thus generating a dipole-like structure. Such a dipole-like beam proves to be better suited for exciting spatial gap solitons arising from the edge of the Brillouin zone of the first band, because such solitons possess an inherent staggered structure. Then, we adjust the distance between the cylindrical lens *CL* and the input microscope lens L_1 (40× magnification), so that the input beam into the waveguide array *WA* attains an elliptic shape of proper dimensions, thus facilitating the excitation of a well defined number of input channels. We choose the polarization of the input light to be extraordinary with respect to the crystalline axes of the $LiNbO_3$ crystal, thus using its largest electrooptic coefficient r_{33}. In all our experiments, we maintain a constant value for the beam diameter in the non-periodic direction of ~2.5 μm (FWHM), fitting nicely to the diffusion depth of each channel waveguide. On the other hand, in the direction of the grating vector, we use various beam diameters in the range from 4 to 100 μm. We vary the propagation angle of the input beam by moving the input lens L_1 perpendicular to the beam. Alternatively, in some cases we use a rotatable thick glass plate located in front of the cylindrical lens. Finally, at the end face of the array we use another microscope lens L_2 (20× magnification) to image the light distribution onto a CCD camera.

3. Fundamentals

Scalar paraxial wave propagation in a nonlinear 1D waveguide array is described by

$$i\frac{dE}{dy} + \frac{1}{2k}\frac{d^2E}{dz^2} + k\left(\frac{n(z)+\Delta n}{n}\right)E = 0 \ . \qquad (1)$$

Here, *E* is the amplitude of the electric light field, $k = 2\pi n/\lambda$ and *n* are the wave number and refractive index of the light in the substrate, $n(z)$ is the periodically-modulated refractive

#6929 - $15.00 US Received 22 March 2005; revised 18 May 2005; accepted 24 May 2005
(C) 2005 OSA

index defining the waveguide array, and Δn is the nonlinear refractive index change ($|\Delta n| << n$). In this equation, y is the propagation direction and z is the transverse coordinate (x is the "depth" coordinate and does not play any role here; see also sketch in Fig. 2). We use this notation to conform the definition of the crystalline axes of $LiNbO_3$. The photovoltaic nonlinearity giving rise to Δn is of saturable form [32,34,35]

$$\Delta n = -\frac{1}{2} n^3 r E_{pv} \frac{I}{I + I_d} \ , \tag{2}$$

with r being the electrooptic coefficient, E_{pv} the (light-induced) photovoltaic field, I the light intensity, and $I_d = G/s$ being the dark irradiance, with a dark generation rate G and a photo-ionization cross-section s. The specific parameters for extraordinarily polarized light in $LiNbO_3$ are $n = 2.242$ and $r = r_{33} = 30$ pm/V. Photovoltaic fields in copper-doped $LiNbO_3$ have been found to reach values of about $E_{pv} = 7$ kV/mm for copper concentrations of $c_{Cu} = 50\times10^{24}$ m^{-3} [44], resulting in a maximum nonlinear refractive index change of $\Delta n \approx 10^{-3}$. This value may be considerably lower for smaller total copper concentration and samples that have been reduced by annealing treatment, i.e. that have a smaller concentration of Cu^{2+}.

We investigate first the band structure of the periodic waveguide array. To do that, we solve the linear version of Eq. (1) (with $\Delta n = 0$, corresponding to a vanishing low intensity), seeking solutions of the form $E(y,z) = A(z)\exp(i\beta y)$ with mode amplitude A and propagation constant β. Then, following the translation symmetry $n(z) = n(z+\Lambda)$, we apply the Floquet-Bloch theorem and seek solutions of the form $A(z) = U(z)\exp(iK_z z)$, where K_z is the transverse wave number and $U(z) = U(z+\Lambda)$ is a periodic function. This leads to

$$\frac{1}{2k}\frac{d^2U}{dz^2} + \frac{iK_z}{k}\frac{dU}{dz} - \frac{K_z^2}{2k}U + k\frac{n(z)}{n}U = \beta U \ . \tag{3}$$

This equation can be solved numerically for the eigenvalue β as a function of the transverse Bloch wave number $K_z \in [-\pi/\Lambda, \pi/\Lambda]$ giving the diffraction/dispersion relation (band structure) of the periodic medium, where allowed values of the propagation constant β are separated by band-gaps. After solving for the linear Bloch modes of the system and obtaining its transmission spectrum, we investigate nonlinear propagation and the formation of 1D lattice solitons by solving Eq. (3) with ($n(z) + \Delta n$) replacing $n(z)$.

4. Results and discussion

We first carry out the "benchmark experiment" described in Section 1, by launching a low intensity light beam, of 4 μm (FWHM) horizontal width, into a single waveguide channel at normal incidence ($K_z = 0$). A photograph of the output intensity is shown at the top of Fig. 3. Clearly, the output intensity distribution is symmetric about the excited channel, covering 35 channels, and possesses the characteristic twin lobes on such an experiment [3]. The input power in this experiment is chosen to be low and the output photograph is taken immediately after switching on the input light, so as to avoid any nonlinear effects that develop in this material rather slowly. For comparison, we also simulate the beam propagation in the waveguide array using a 4th-order FFT beam propagation method (BPM) [45]. The calculated propagation results are shown at the bottom of Fig. 3, and they display a good agreement with the experimental results.

Staying within the linear case, we calculate the transmission spectrum of the 1D array and find the expected band structure shown in Fig. 4. To apply the 1D theoretical model to our 2D channel waveguide array, we use the value of the periodic index change at the proper "depth" coordinate x discussed in section 2 (see also Fig. 1).

#6929 - $15.00 US Received 22 March 2005; revised 18 May 2005; accepted 24 May 2005
(C) 2005 OSA

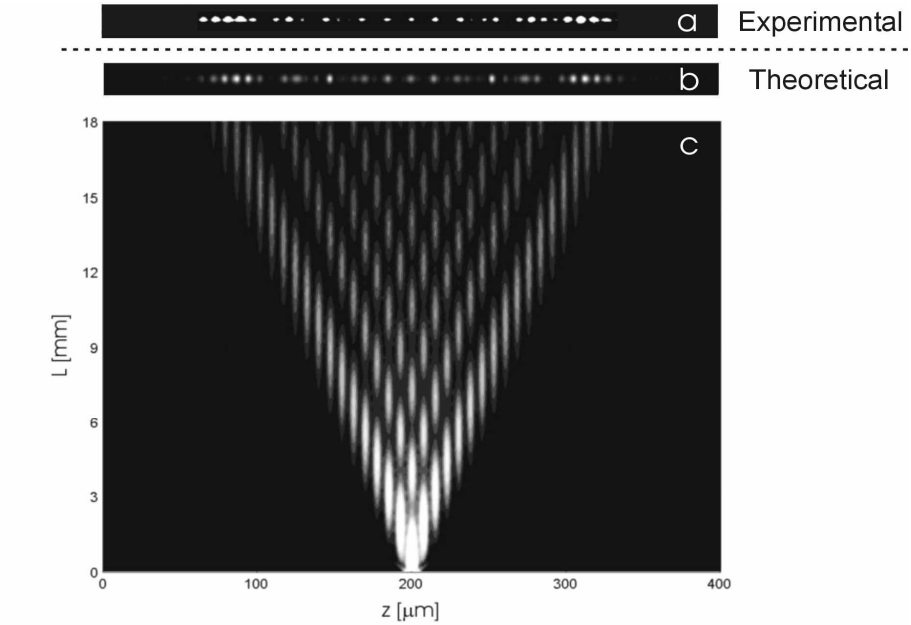

Fig. 3. Experimental (a) and theoretical (b,c) results showing discrete diffraction of light in a $LiNbO_3$ waveguide array, when a single input channel is excited. The upper part in (a) shows the intensity distribution at the output of the waveguide array, as photographed with a CCD camera. The two lower parts (b) and (c) show the simulated propagation of a beam in a waveguide array under the same parameters, at the "depth" of the maximum intensity of each individual mode.

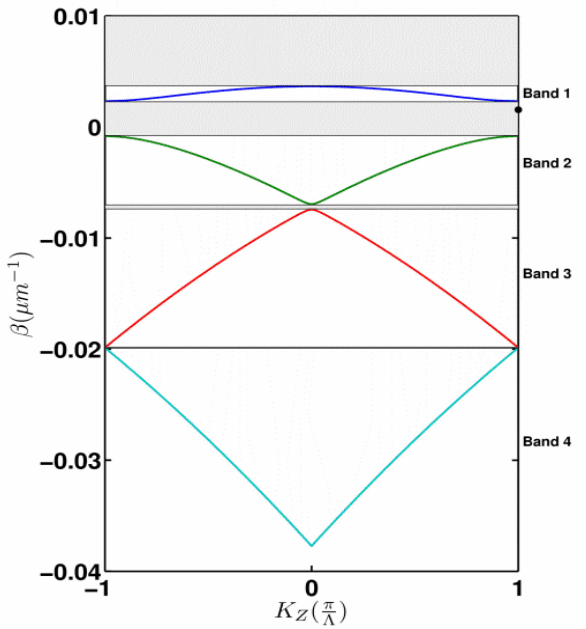

Fig. 4. Band-gap diagram of the waveguide array, relating the propagation constant β to the Bloch wave number K_z as described in section 2. The value "0" corresponds to a plane wave propagating in the substrate. The shaded regions represent the gaps where light propagation is forbidden. The black dot at the edge of the first band indicates the propagation constant of the gap soliton (shown in Fig. 7). Increasing the optical intensity creates a negative defect in the periodic structure, thereby localizing the corresponding Bloch wave by pushing its propagation constant β down into the gap, thus converting it from an extended Bloch wave into a self-localized state: a gap soliton.

#6929 - $15.00 US
Received 22 March 2005; revised 18 May 2005; accepted 24 May 2005
(C) 2005 OSA

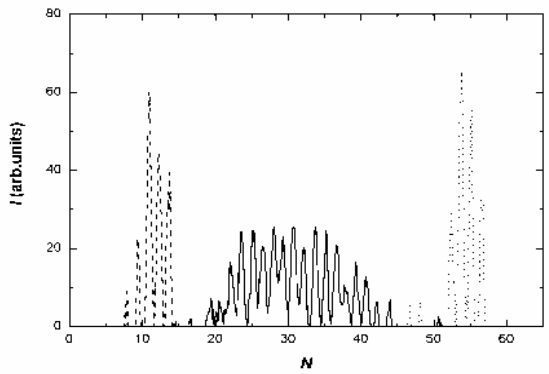

Fig. 5. Probing diffraction in the periodic waveguide array by varying the angle of incidence of a four-channel input beam, from K_z = 0 (solid line), to nearly diffraction-free propagation at $K_z \approx \pm\pi/2\Lambda$ (dotted and dashed lines).

Then, we change the angle of incidence of the input light beam, scanning the launch angle over the first Brilluoin zone, from $K_z = 0$ to $K_z \approx \pi/\Lambda$. Subsequently, diffraction varies from being normal, to almost no diffraction, and then to being anomalous [46,47]. To experimentally demonstrate almost diffraction-free propagation at $K_z \approx \pi/2\Lambda$, we launch an input beam with a width (FWHM) of 30 μm, exciting roughly four channels of the array. As shown by the intensity profiles in Fig. 5, which are taken from the output face of the array, for a normal-incidence input beam with K_z = 0 (solid line), the beam broadens considerably into roughly 20 channels. When the incidence angle is at $K_z \approx \pm\pi/2\Lambda$ (dashed and dotted lines, respectively), the output beam is almost diffraction-free occupying roughly four channels.

Then, we move on to the anomalous diffraction region, launching the input beam at the Bragg angle ($K_z \approx \pi/\Lambda$). This is also where we can form first-band bright solitons in such nonlinear medium, because the photovoltaic nonlinearity in $LiNbO_3$ is of the self-defocusing type. Such solitons, arising from the Bloch wave at the edge of the first Brilluoin zone, have a staggered phase structure, and their propagation constant lies within the first gap (between the first and second transmission bands). Thus, such solitons are often called "spatial gap solitons" or "staggered solitons" [4-7]. The solitons form when the optical intensity is sufficiently high so that the propagating light beam induces (through the self-defocusing nonlinearity) a negative defect in the periodic index structure. When the beam has a structure close enough to the structure of the bound state of the induced defect, the optical beam self-traps in its own induced defect, thereby forming a spatial gap soliton.

Experimentally, to facilitate efficient excitation of a Bloch mode propagating close to the edge of the Brillouin zone ($K_z = \pi/\Lambda$), we divide the input light beam into two parts using the tilted thin glass plate (see Fig. 2) that covers half of the beam, thus creating a dipole with a relative phase of π. This beam is then carefully adjusted to be launched, at normal incidence, into two neighboring waveguides, with a total input power of ≈16 μW. The idea behind this method is to generate an input beam that has a larger overlap with the amplitude profile of a gap soliton arising from the edge of the Brillouin zone of the first band. Such solitons have the "phase signature" of the Bloch mode associated with the same transverse momentum [6]. Our excitation method facilitates a larger overlap with the gap soliton $K_z = \pi/\Lambda$ wavefunction. At the same time, our method avoids difficulties associated with setting two-beam interference to generate nn appropriate input beam, which then has to be matched carefully to the lattice. The response time of the photovoltaic nonlinearity in our sample is rather long (≈1 hour) [48], thus we monitor the intensity distribution of the beam exiting the array as it evolves in time, eventually forming a spatial gap soliton. Consequently, we monitor the linear propagation of the input beam through the waveguide by monitoring the

#6929 - $15.00 US Received 22 March 2005; revised 18 May 2005; accepted 24 May 2005
(C) 2005 OSA

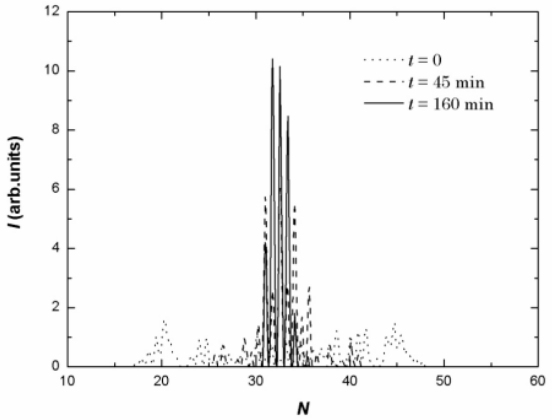

Fig. 6. Formation of a gap soliton in a 1D $LiNbO_3$ waveguide array. The figure shows a line scan of the light intensity distribution measured by a CCD at the output facet of the array, where the dotted, dashed and solid lines represent the intensity profile at times $t \approx 0$, t = 45 min, and t = 160 min, respectively.

intensity distribution at the sample's output face immediately after switching on the light. This output intensity distribution is shown for linear propagation at $K_z = \pi/\Lambda$ in Fig. 6 (dotted line). After several minutes of illumination, the pattern starts to narrow (dashed line) by the action of the self-defocusing photovoltaic nonlinearity. Finally, the output intensity distribution reaches steady state (solid line) which does not change its intensity profile even after several hours. This structure is a spatial gap soliton. We compare these experimental

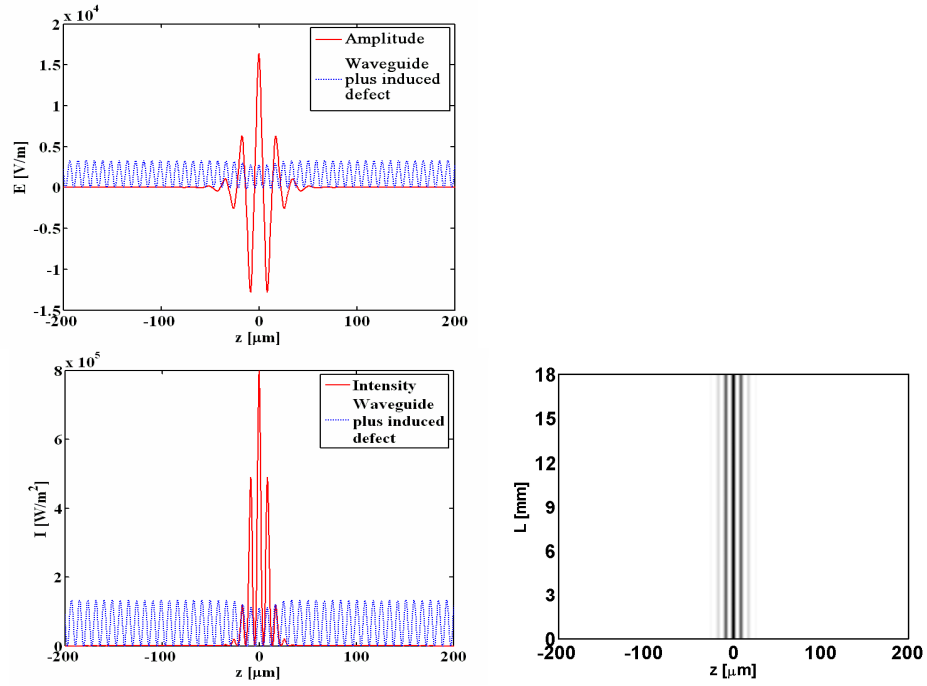

Fig. 7. Calculated wavefunction and propagation dynamic of a spatial gap soliton in our setting. Left and middle panels: amplitude and intensity of a gap soliton (solid line) plotted on the background of the waveguide structure with the light-induced (negative) defect the soliton creates (dotted lines). Right panel: simulated stable and stationary propagation of the gap soliton in the waveguide array. The intensity profile of the soliton shown propagating in the right panel corresponds to the intensity of the soliton shown on the left panel.

#6929 - $15.00 US Received 22 March 2005; revised 18 May 2005; accepted 24 May 2005
(C) 2005 OSA

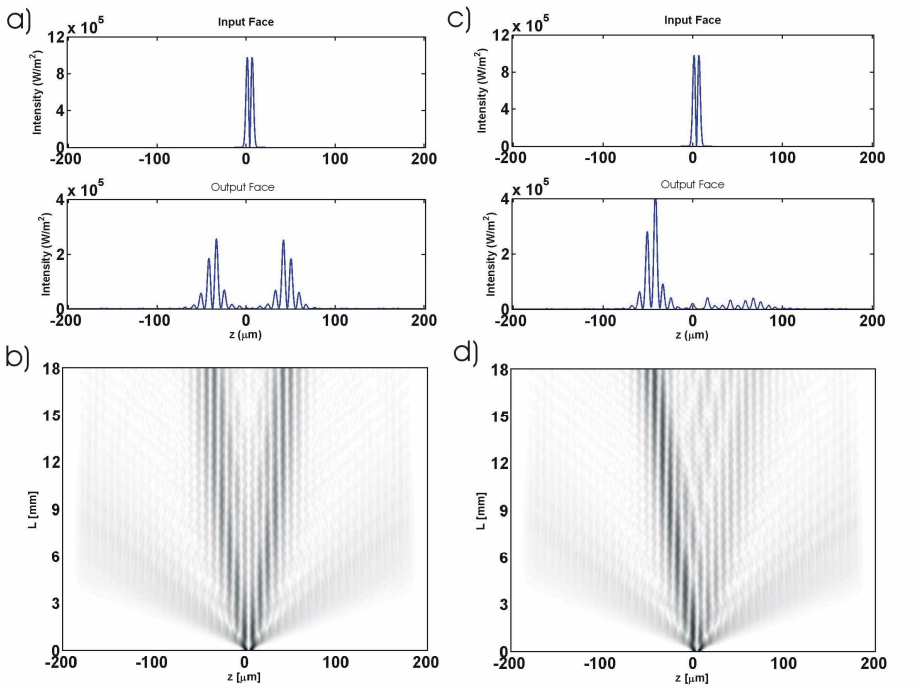

Fig. 8. Numerical results for the nonlinear propagation of a Gaussian beam with a π phase jump at its center (a dipole): a), b), the beam is launched normal to the waveguide array, and c), d), the same input beam is launched with a tilt of 2 mrad into the array. In both cases the input power is 16 μW and the input beam covers about half a lattice constant (FWHM of the Gaussian beam of 4.2 μm).

results with the theory, and find in Fig. 7 that the calculated amplitude and intensity (left and middle diagrams, solid lines) and simulated propagation (right diagram) of such a gap soliton in a sample with 50 channel waveguides, under the same parameters as used in the experiment, occupies roughly 5 channels, and exhibits stable stationary propagation in the waveguide array. The experimental results are in good agreement with the simulation.

To simulate our experiment, we propagate a Gaussian beam ($x \exp(-x^2)$ with a π phase jump at its center (a dipole). The beam's FWHM is half a lattice constant (4.2 μm), it is centered between two waveguides, and its input power is 16 μW. When the beam is launched exactly normal to the waveguide array, two staggered solitons are created propagating in opposite directions. As the two solitons propagate, their transverse velocities decrease (see Figs. 8(a), (b)). However, when the beam is launched with some minor tilt (in our simulation: 2 mrad which is 1/6 of the angle to the edge of the first Brillouin zone), the power is divided unevenly between the two lobes of the beam. As a consequence, only one staggered soliton is created from the intense lobe, while the second lobe of the beam, being underpowered, radiates slowly its energy and disappears (see Figs. 8(c), (d)). In this process, approximately a quarter of the beam's initial power was radiated and the surviving soliton's power is approximately 12 μW. In our experiments, we generally observe only a single gap soliton (similar to Fig. 8(d)), and not the soliton pair. Apart from a very small asymmetry in the incoupling geometry (small tilt angle, slightly unequal intensity in the two lobes), which hardly can be avoided, the reason is, most likely, higher order terms in the photovoltaic nonlinearity that break the symmetry [49], having an effect similar to that of the small tilt angle. Most probably, in order to experimentally observe the soliton pair evolving from a normal-incidence dipole-type beam, one would have to have a highly symmetric nonlinearity for which $\Delta n(z) = \Delta n(-z)$.

#6929 - $15.00 US Received 22 March 2005; revised 18 May 2005; accepted 24 May 2005
(C) 2005 OSA

Summary

We have investigated linear and nonlinear propagation of light in a 1D waveguide array possessing a saturable self-defocusing nonlinearity arising from the bulk photovoltaic effect in $LiNbO_3$. For low input power, discrete diffraction is observed, whereas for higher input powers, the build-up of a negative nonlinear index change allows for the formation of bright gap solitons that have a propagation constant within the gap of the linear dispersion spectrum. Experimentally, such a "staggered" bright gap soliton is observed when two wave packets with a relative phase difference of π are used to excite, at normal incidence, two adjacent waveguides at the input face. The diffraction properties of our sample are modelled using Floquet-Bloch waves and calculating the corresponding band-gap structure. These numerical calculations confirm our experimental results and show a stable propagation of gap solitons in the array. This is to our knowledge the first observation of lattice solitons supported by the photovoltaic nonlinearity.

Acknowledgments

This work was supported by the German-Israeli DIP project, through the German Federal Ministry of Education and Research (BMBF, grant DIP-E6.1). F. Chen gratefully acknowledges the Alexander von Humboldt Foundation for financial support.

#6929 - $15.00 US Received 22 March 2005; revised 18 May 2005; accepted 24 May 2005
(C) 2005 OSA